Ahliya Journal of Allied Medico-Technology Science
[Published by Palestine Ahliya University]
Vol. 01 Issue 02 (2024)
ISSN: 3007-9489

Radiation Shielding Efficacy of Barium Oxide Doped Borosilicate Glass: Monte Carlo Simulation Study

Bassam M. Abunahe[1], Iskandar Shahrim Mustafa[1], Efenji Godwin[1], Ahmad Umar Ahmad[1], Mohamad Aminudin Said[2]

[1] School of Physics, Universiti Sains Malaysia (USM), 11800, Gelugor, Pulau Pinang (Malaysia)
[2] Nuclear Medicine Department, Institut Kanser Negara, Presint, 62250, Putrajaya (Malaysia)
✉ iskandarshah@usm.my

Received:23/10/2024 Accepted:15/11/2024 Published:15/12/2024

Abstract: ***Radiation is a type of energy that emitted from a source, transferred through space, and interacted by a material. Ionizing radiation can cause damaged for human health which lead to genetic mutations or even death. Shielding is one of the cardinal rules of radiation protection. Recently, different types of glass surged as a possible radiation shielding material. Borosilicate glass doped with high metal oxides increased the radiation shielding efficacy of the glass. The difficulty in performing the experimental work in terms of equipment availability as well as the validity of that work leads to the field of simulation and modelling. This study aims to simulate the measurement process of radiation shielding of bismuth- zinc-borosilicate glass, which is doped with different mole percentage (mol%) of barium oxide. Also, the radiation shielding efficiency is examined using three radioactive sources (99m Technetium, 137 Cesium, and 60 Cobalt). Using Geant4/ Gate simulation code, the energy deposited was incrementally decreased as the doping mol% of barium oxide increased from 0 – 15 mol%. The lowest energy deposited obtained with the highest doping percentage of barium oxide (15 mol%) and photon energy (1.332 MeV). This study validates an experimental study which suggest the use of barium oxide doped bismuth-zinc-borosilicate glass as a gamma shielding material.***

Keywords: ***Borosilicate Glass; Simulation; Radiation Shielding; Barium Oxide.***

1. Introduction

Radiation, as an energy emitted from a source, travel through space and possesses the capability of material penetration. Given its widespread applications, radiation emerges as a significant area of concern. Prolonged exposure to radiation can result in genetic alterations or even death. One of the cardinal rules of radiation protection is shielding. Different types of shielding materials have been widely used for different radiation types [1-3].

Concrete and lead are the two most often radiation shielding materials. However, lead is toxic and uncertainty in dose calculation with concrete increased the demand for a substitute shielding material [4-6]. Recently, different glass materials surged as a sustainable radiation shielding material. This includes silicon oxide (SiO2), boron oxide (B2O3), phosphorus oxide (P2O5), tellurium oxide (TeO2), Antimony oxide (Sb2O3), and germanium oxide (GeO2) [7-9].

Borosilicate glass doped with high metal oxides (barium, bismuth, or tungsten oxides) surged as potential radiation shielding material [10-14]. The efficiency of any type of shielding material involves two approaches: experimental measurement or modelling using specific particle transport simulation code. The experimental work is a time consuming and some challenges rise from the need for highly accurate measurements, which must account for the unique geometries and mechanical properties of the investigated object. Meanwhile, modelling is a flexible and straightforward technique that allows for easy application [15].

Different simulation codes were applied in literature including GEANT4, FLUKA, and MCNPX. Different studies used Geant4 to validate the radiation shielding efficiency of their fabricated borosilicate glass. For instance, at 0.347 MeV gamma energy using Geant4 code, borosilicate glass doped with 5 mol% of Bi2O3 achieved lower HVL of 1.44 cm than those doped with 5 mol% of BaO (HVL = 2.49) or TiO2 (HVL = 2.62 cm) [16]. This was referred to high $Mw$of Bi2O3 (465.96g/mole) when it compared with BaO (Mw =153.33g/mole) or TiO2 (Mw = 79.866 g/mole). Meanwhile, using MCNP code, borosilicate glass doped with BaO 30 mol% at 1.408 MeV gamma energy, had achieved the lowest HVL of 2.7 cm with μρ of 0.15 cm2/g [17]. At higher energy level of 15 MeV gamma energy, borosilicate glass doped with 40 mol% of BaO, had the lowest HVL of 7 cm with μρ of 0.029 cm2/g using MCNP simulation code. Also, it had better neutron shielding with $\sum R$ of 0.0994 cm^{-1} compared with graphite ($\sum R$ = 0.094 cm−1) and ordinary concrete ($\sum R$ =0.077 cm^{-1}) [18].

Moreover, borosilicate glass doped with 2mol% of BaO had achieved the lowest HVL of 12.5 cm with μρ of 0.022 cm2/g using four different simulation codes including Luka, Geant4, MATLAB, and XCOM [19]. This study aims to validate the radiation shielding efficiency for previous experimental study [20, 21]. Borosilicate glass doped with different doping percentages of barium oxide at different gamma energies were evaluated. The energy deposited used for evaluating the radiation shielding efficiency of the glass system.

2. Materials and Methods

Geant 4 simulation code (version 8.2) was used to estimate the energy deposited in sodium oxide scintillation detector. Bi2O3-ZnO-borosilicate glass was used as ternary glass network. The energy deposited was calculated in two different stages. The first stage is using four different doping percentage of barium oxide (i.e., 0, 5, 10, and 15 mol%) at 140 keV monoenergetic gamma emitted from Technetium radioactive source with 1000 Becquerel activity.

The second stage is using borosilicate glass doped with 15 mol% of BaO at four different monoenergetic gamma energies including 0.140, 0.662, 1.173, and 1.332 MeV emitted from 99m Technetium (99mTc), 137 Caesium (137 Cs), and 60 Cobalt (60 Co), respectively. The simulation set up composed of mother volume of 5 m x 5 m x 5 m box of air. The daughter volume, where the internal system of glass sample, lead blocks, radioactive source, and sodium iodide NaI (TI) scintillation detector inserted. It was a box of air volume with 300 cm x 300 cm x 300 cm. Inside the daughter volume, four-cylinder lead blocks were inserted. The dimensions of each block and the scintillation detector were identical with 6.9 cm maximum radius and 20 cm length. The position of lead block was centred so it shields the radioactive source, glass sample, and the entrance of the detector. The glass sample is cylinder in shape with 0.5 cm maximum radius and 2 cm and length. The radioactive source with an activity of 1000 becquerel was cylindrical in shape with I cm radius and 1 cm half of length. The type of gamma emission was isotopic. The total number of primaries was 100 times. Figure 1 illustrates the simulated set up. The mole percentage of the component of the simulated borosilicate glass samples is summarized in Table1

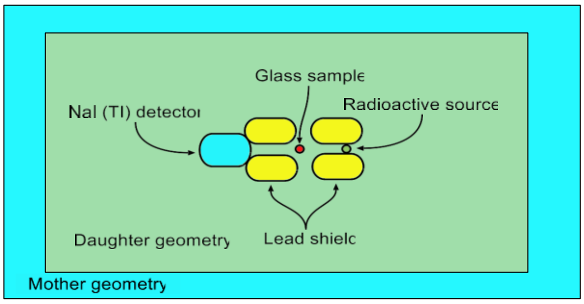

Figure 1. Schematic illustration of simulation modelling set up.

Table1. Mole percentage of component of borosilicate glass samples

Sample	BaO mol%	Bi2O3 mol%	ZnO mol%	B2O3 mol%	SiO2 mol%
S1	0.000	0.200	0.300	0.200	0.300
S2	0.050	0.200	0.300	0.162	0.300
S3	0.100	0.200	0.300	0.125	0.300
S4	0.150	0.200	0.300	0.05	0.300

3. Results and Discussion

The simulation setup and initiation of radioactive source is presented in Figure 2. The effect of variation of barium oxide mol% as well as the gamma energies on the energy deposited are illustrated in Figure 3 and 4. Also, the effect of increasing gamma energy on the interaction of the photon with the glass sample and inside the detector is demonstrated in Figure 5.

3.1 Simulation setup and radiation initiation

Figure 2(a) demonstrates the actual modelling of the set up. The radioactive source (blue) emitted the gamma rays isotopically and interacts with the borosilicate glass sample (red) before being detected by the scintillator (cyan). All of the scatted radiation emitted as a result of sample or detector interaction was absorbed by the lead blocks (below). Figure 2(b) demonstrates the simulation setup after running the radiation source where the gamma ray (green) interacts with the glass sample (red) and the attenuated rays detected by the detector. As shown in the Figure 2(b) all of the backscattered radiation due to the interaction of the incident gamma ray with the glass sample are being absorbed by the lead blocks.

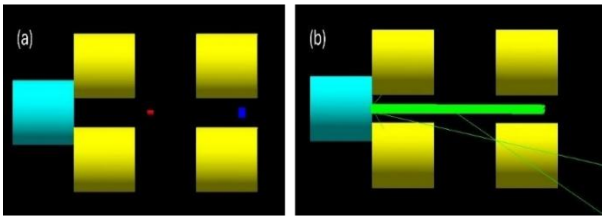

Figure 2.Geant 4 modelling set up (a) before running the radiation source, (b) after running monoenergetic gamma photons from gamma emitter radioactive source with different energies.

3.2 Effect of barium oxide doping percentage on the energy deposed

The amount of energy deposited with the variation of doping percentage of barium oxide from 0 – 15 mol% is illustrated in Figure 3. It is noticed that as the BaO mol% increased, the energy deposited decreased, due to the higher density of the borosilicate glass, so more photon attenuation (absorption or scattering) occurred, so less photon detected. As the photon energy examined with the different mol% BaO is in the diagnostic range (140 keV), the photoelectric absorption is the predominant photon interaction in this range. This means that almost all of the incident photon energy is absorbed by the glass sample. This is because with this interaction, most of the incident photon energy is equal to or slightly higher than energy of the electrons in the most inner shell (K or L shell) in the glass system. The reported reduction in the energy deposited is also referred to the increased sample density as the BaO mol% increased from 0 – 15 mol%. This reduction in the borosilicate glass density is due to the replacement of boron with low atomic weight (Mw =10.82 g/mol) with higher molecular weight atom (Mw = 153.33 g/mol). Additionally, because of the high atomic number of barium (Z=56) the probability of photoelectric absorption increase, as it inversely proportional with the Z3. Our result is in good agreement with an experimental result reported by Thair et al. [20, 21]. They reported an incremental increase in the mass attenuation coefficient, effective atomic number, and effective electron density as the BaO mol% increased from 0-5%.

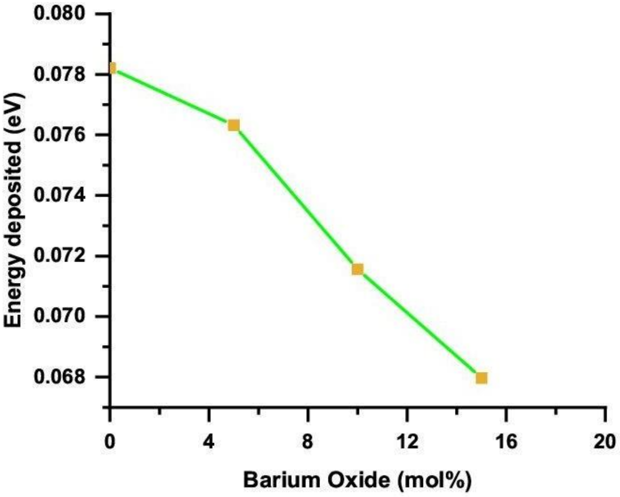

Figure 3. Energy deposited (eV) with 140 keV gamma photon as a function of BaO mol%.

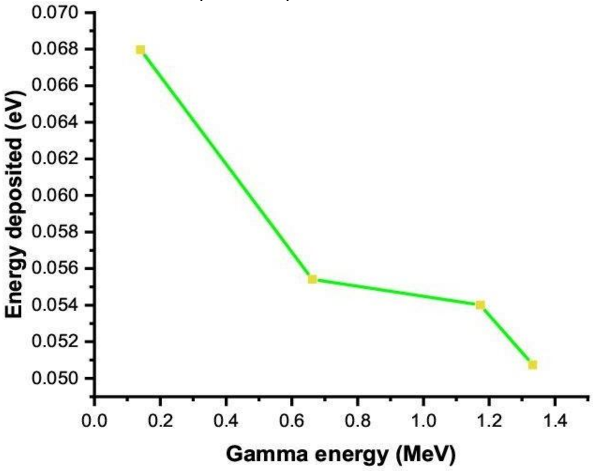

Figure 3. Energy deposited (eV) with 140 keV gamma photon as a function of BaO mol%.

3.3 Effect of gamma energy on the energy deposed

The amount of energy deposited with the variation of gamma energy from 0.140 – 1.332 MeV with the glass sample doped with 15 mol% BaO is demonstrated in Figure 4. As shown from the Figure, that as the photon energy increased from 0.140 – 1.332 MeV, the energy deposited inside the scintillation detector decreased from 0.07463 – 0.05437 eV. This is logically true, since as the photon energy increases, the probability of photon interaction and losing its energy decreased. As photon energy increased, the probability of Compton scattering and pair production interactions increased. The probability of Compton scattering is directly proportional with the electron density of material and inversely with the atomic number [19, 22].

As can see from Figure 5 (a – d) that as the photon energy increased from 0.140 – 1.332 MeV, the gamma photon became more penetrating and interacting deeper inside the detector, so with increasing the photon energy, lesser energy will be deposited inside the detector. Moreover, with increasing the energy most of the scattered radiation become forward scattering. As it shown in Figure 5 (d), almost all of the scattered radiation due to the interaction of gamma ray of 1.332 MeV was towards the detector compared with lower gamma energies, where backscattered radiation was reported as shown in Figure 5(d). Finally, with higher photon energy, the probability of photon interaction will no longer depends on the atomic number of the material. This is obvious from Figure 5 (a – d) that will be increasing the energy, the glass sample attenuate the incident photon, but with higher energy, no more effect of glass sample on the attenuation. So, this give an indication, that this bismuth-zinc-borosilicate glass doped with 15 mol% of BaO is more effective than other samples to be applied as shielding material in lower gamma energy levels (less than 0.140 MeV) due to the highest energy deposited inside the detector [23].

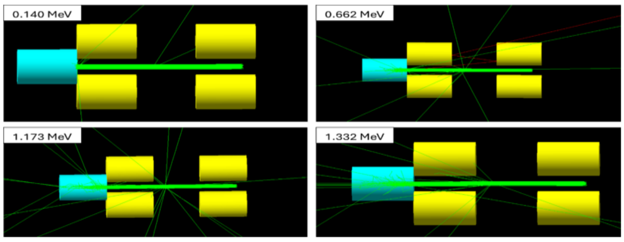

Figure 4. Figure. 5 Energy deposited (eV) as a function of gamma photon energy.

4. Conclusion

Radiation is a type of energy emitted from a source, travels through space, and interacts with materials. Ionizing radiation poses health risks, including genetic mutations and death. Shielding is vital for radiation protection. Borosilicate glass doped with high metal oxides had been applied as radiation shielding material. The radiation shielding efficiency of borosilicate glass was examined at different gamma energies (0.140 – 1.332 MeV) and doping percentage of barium oxide (0 – 15 moles%). Using Geant4/ Gate simulation code, the energy deposited was incrementally decreased as the doping mol% of barium oxide increased from 0 –15 mol%. The lowest energy deposited obtained with the highest doping percentage of barium oxide (15 mol%) and photon energy (1.332 MeV). This validates an experimental study which suggest the use of barium oxide doped bismuth-zinc-borosilicate glass as a gamma shielding material.

Reference

[1] Akkurt, I., et al., Chemical corrosion on gamma-ray attenuation properties of barite concrete. Journal of Saudi Chemical Society, 2012. 16(2): p. 199-202.

[2] Sharifi, S., R. Bagheri, and S. Shirmardi, Comparison of shielding properties for ordinary, barite, serpentine and steel–magnetite concretes using MCNP-4C code and available experimental results. Annals of Nuclear Energy, 2013. 53:p. 529-534.

[3] Shirmardi, S., M. Shamsaei, and M. Naserpour, Comparison of photon attenuation coefficients of various barite concretes and lead by MCNP code, XCOM and experimental data. Annals of Nuclear Energy, 2013. 55: p. 288-291.

[4] AbuAlRoos, N.J., N.A.B. Amin, and R. Zainon, Conventional and new lead-free radiation shielding materials for radiation protection in nuclear medicine: A

review. Radiation Physics and Chemistry, 2019. 165: p. 108439.
[5] Manohara, S., S. Hanagodimath, and L. Gerward, Photon interaction and energy absorption in glass: a transparent gamma ray shield. Journal of Nuclear materials, 2009. 393(3): p. 465-472.
[6] Kurudirek, M., et al., Comparison of some lead and non-lead based glass systems, standard shielding concretes and commercial window glasses in terms of shielding parameters in the energy region of 1 keV–100 GeV: a comparative study. Journal of nuclear materials, 2010. 407(2): p. 110-115.
[7] Singh, K., et al., Gamma-ray shielding and structural properties of PbO–SiO2 glasses. Nuclear Instruments and Methods in Physics Research Section B: Beam Interactions with Materials and Atoms, 2008. 266(6): p. 944-948.
[8] Singh, N., et al., Comparative study of lead borate and bismuth lead borate glass systems as gamma-radiation shielding materials. Nuclear Instruments and Methods in Physics Research Section B: Beam Interactions with Materials and Atoms, 2004. 225(3): p. 305-309.
[9] Darwish, A., S.A. Issa, and M. El-Nahass, Effect of gamma irradiation on structural, electrical and optical properties of nanostructure thin films of nickel phthalocyanine. Synthetic Metals, 2016. 215: p. 200-206.
[10] Sayyed, M., et al., Structural, optical, and shielding investigations of TeO 2– GeO 2–ZnO–Li 2 O–Bi 2 O 3 glass system for radiation protection applications. Applied Physics A, 2019. 125: p. 1-8.
[11] Abouhaswa, A., et al., Physical, structural, optical, and radiation shielding properties of B2O3-20Bi2O3-20Na2O2-Sb2O3 glasses: Role of Sb2O3. Journal of Non-Crystalline Solids, 2020. 543: p. 120130.
[12] Alajerami, Y., et al., Physical, structural, and shielding properties of cadmium bismuth borate-based glasses. Journal of Applied Physics, 2020. 127(17).
[13] Khodadadi, A. and R. Taherian, Investigation on the radiation shielding properties of lead silicate glasses modified by ZnO and BaO. Materials Chemistry and Physics, 2020. 251: p. 123136.
[14] Uosif, M.A.M., et al., Structural, mechanical and radiation shielding properties of newly developed tungsten lithium borate glasses: an experimental study. Journal of Non-Crystalline Solids, 2020. 532: p. 119882.
[15] Salama, E. and A. Maher. Application of GATE/GEANT 4 code in investigation of gamma shielding effectiveness of glass materials. in Journal of Physics: Conference Series. 2019. IOP Publishing.
[16] Al-Hadeethi, Y. and M. Sayyed, Analysis of borosilicate glasses doped with heavy metal oxides for gamma radiation shielding application using Geant4 simulation code. Ceramics International, 2019. 45(18): p. 24858-24864.
[17] Mhareb, M., et al., Morphological, optical, structural, mechanical, and radiation- shielding properties of borosilicate glass–ceramic system. Ceramics International, 2022. 48(23): p. 35227-35236.
[18] Tekin, H.O., et al., Nuclear radiation shielding competences of barium- reinforced borosilicate glasses. Emerging Materials Research, 2020. 9(4): p. 1131-1144.
[19] Kilicoglu, O., et al., Nuclear radiation shielding performance of borosilicate glasses: Numerical simulations and theoretical analyses. Radiation Physics and Chemistry, 2023. 204: p. 110676.
[20] Khazaalah, T.H., et al., Development of novel transparent radiation shielding glasses by BaO doping in waste soda lime silica (SLS) glass. Sustainability, 2022. 14(2): p. 937.
[21] Khazaalah, T.H., I.S. Mustafa, and M. Sayyed, Radiation parameterizations and optical characterizations for glass shielding composed of SLS waste glass and lead-free materials. Nuclear Engineering and Technology, 2022. 54(12): p. 4708-4714.
[22] Kaçal, M.R., et al., Gamma shielding and compressive strength analyses of polyester composites reinforced with zinc: an experiment, theoretical, and simulation-based study. Applied Physics A, 2020. 126: p. 1-15.
[23] Kurtulus, R., T. Kavas, and M. Al-Buriahi, A transparent bismo-borosilicate glass against ionizing photons: synthesis and physical, structural, optical, and radiation shielding properties. Journal of Materials Science: Materials in Electronics, 2023. 34(8): p. 7